Science of the Total Environment 867 (2023) 161374

Contents lists available at ScienceDirect

Science of the Total Environment

journal homepage: www.elsevier.com/locate/scitotenv

Decrypting the stream periphyton physical habitat of recently deglaciated floodplains

Matteo Roncoroni [a,*], Davide Mancini [a], Floreana Miesen [a], Tom Müller [a], Mattia Gianini [a], Boris Ouvry [c], Mélanie Clémençon [a], Frédéric Lardet [a], Tom J. Battin [b], Stuart N. Lane [a]

[a] Institute of Earth Surface Dynamics, University of Lausanne, UNIL Mouline, Lausanne, Switzerland
[b] River Ecosystems Laboratory, Alpine and Polar Environmental Research Center Ecole Polytechnique Fédérale de Lausanne (EPFL), Lausanne, Switzerland
[c] Glaciology and Geomorphodynamics group, Physical Geography Division, Department of Geography, University of Zurich, Zurich, Switzerland

HIGHLIGHTS

- Periphyton accrual is controlled by physical disturbances in glacial floodplains.
- The spatial assemblage of disturbances is still poorly understood.
- A set of remote sensing techniques is used to decrypt the physical habitat.
- Disturbances are not spatially homogenous in recently deglaciated floodplains.
- Periphyton may develop in stable streambeds, promoting ecosystem engineering.

GRAPHICAL ABSTRACT

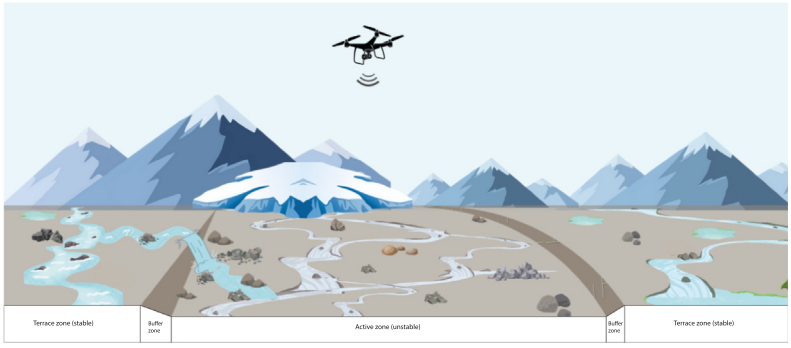

ARTICLE INFO

Editor: Fernando A.L. Pacheco

Keywords:
Periphyton dynamics
Glacial stream habitat
Drones
Photogrammetry
Land-use mapping

ABSTRACT

The rapid recession of glaciers is exposing large zones to the development of embryonic phototrophic ecosystems and eventual ecological succession. Traditionally, succession patterns in glacial forefields have been seen as a response to time since deglaciation, but nowadays forefield exposure is so rapid that this theory may be less applicable. In this succession process, periphyton are potential pioneer organisms because of their role in modifying the local environment (e.g. access to water) to create conditions conducive to plant colonization. In this paper, we aim to decrypt the physical properties of the habitats that define the spatial and temporal assemblage of periphyton during the melt-season of an Alpine temperate glacier in the context of rapid climate change. We show that periphyton develop in glacial floodplains throughout the melt-season and could extend to cover significant surfaces. However, development is only possible when the combined conditions of stability and water accessibility are met. In glacial floodplains, stable zones exist and are typically located on terraces; but they can also be locally found for much shorter periods in the more active, glacial-stream reworked zone. On terraces, water accessibility can be a limit due to well-drained sediments, but when present, often aided by the role that biofilms play in creating an impermeable layer, it provides a stable and clear water source that biofilms could exploit. In the active part of the braid plain, whilst water availability is very high, the water is harsh (low temperature, high turbidity) and erosive. Therein, periphyton can rapidly exploit short windows of opportunity but the habitat conditions rarely remain stable for long enough for continuous periphyton cover to develop. Thus, the role of periphyton in ecosystem succession is strongly conditioned by the spatial extent of the active zone, itself a function of high rates of glacier melt and sediment supply associated with rapid glacier retreat.

* Corresponding author.
E-mail address: matteo.roncoroni@unil.ch (M. Roncoroni).

http://dx.doi.org/10.1016/j.scitotenv.2022.161374
Received 14 November 2022; Received in revised form 21 December 2022; Accepted 31 December 2022
Available online 5 January 2023

1. Introduction

The glacial floodplains that form downstream of Alpine glacier margins are known for being highly unstable during the melt season (Marren, 2005; Heckmann et al., 2016; Miller and Lane, 2019). Such instability is associated with high rates of both glacial melt and subglacial sediment supply (Nienow et al., 1998; Heckmann et al., 2016; Perolo et al., 2019) in the form of both bed and suspended load (Gurnell, 1987; Milner and Petts, 1994; Swift et al., 2005). Due to its high turbidity, the solar radiation reaching the streambed is also attenuated (Boix Canadell et al., 2021). Thus, glacial water is harsh in ecological terms (Gabbud et al., 2019) and this has a significant strong impact on the organisms that inhabit such environments, likely limiting their development and survival (Milner and Petts, 1994).

Despite this unfavorable context, periphyton communities do develop in recently formed glacial floodplains. Uehlinger et al. (1998, 2002, 2010) noted that periphyton biomass is very low during the melt season because disturbance rates are high. Daily discharges are high, commonly high enough to cause shear stresses on the stream bed that exceed the critical shear stresses required for periphyton removal (Biggs and Close, 1989; Biggs et al., 1999; Francoeur and Biggs, 2006; Neumeier et al., 2006; Thom et al., 2015; Hoyle et al., 2017). The suspended load is also high, increasing the probability of abrasion of the periphyton mat (Horner and Welch, 1981; Horner et al., 1990; Francoeur and Biggs, 2006; Luce et al., 2010, 2013); and decreasing the solar radiation available to photosyntetically active microorganisms growing on the stream bed (Uehlinger et al., 2002, 2010). In this context, the time between two disturbances is often significantly shorter than the time needed for periphyton to develop (Thom et al., 2015). However, glacial floodplains are heterogeneous and conditions may develop locally where stability is sufficient to allow periphyton to develop (Roncoroni et al., 2022), possibly aided by the ecosystem engineering provided by the periphyton themselves (Miller and Lane, 2019; Roncoroni et al., 2019).

Glacial floodplains are drained by a set of water sources, which are not limited to glacial sources alone (Malard et al., 1999; Ward et al., 1999; Müller et al., 2022); both krenal and rhithral sources may be present (Malard et al., 1999; Ward et al., 1999). These sources are less harsh as compared to glacial water due to their negligible turbidity and relative hydrological and thermal stability (Uehlinger et al., 1998; Boix Canadell et al., 2021). Provided that glacial water does not intrude into these channels during the melt season, krenal and rhithral sources offer more benign conditions and allow periphyton to develop (Uehlinger et al., 1998; Brandani et al., 2022). However, they are also prone to progressive drying during the melt season where they are dependent upon snow-melt as it becomes progressively exhausted.

Glacial floodplains are also characterized by zones of geomorphic stability that vary in space and time. Terraces are common in glacial floodplains (Germanoski and Schumm, 1993; Marren, 2002; Marren and Toomath, 2013, 2014; Roussel et al., 2018), and are rarely if never inundated by glacial water (Roncoroni et al., 2019). The morphological disconnection from the more active floodplain makes terraces extremely stable yet prone to dry conditions if not connected to krenal and rhithral sources (Malard et al., 1999; Ward et al., 1999). Within the more active floodplain, stream braiding is common (Maizels, 2002; Marren, 2005) and likely results in a wider distribution of bed shear stresses and water depths (Bakker et al., 2019). Braiding intensity also evolves through time, and when it is high bedload tends to be reduced (Ashmore, 1988; Ashmore et al., 2011) or focused on a few very active channels where the bulk of water flows preferentially (Bertoldi et al., 2009; Egozi and Ashmore, 2009). This, in turn, has the result that some braids become less harsh for short periods time.

This review emphasizes that the development of periphyton during the melt season likely reflects the balance between the mosaic of heterogeneous yet-interconnected habitats and their stability within the glacial floodplain (Ward et al., 1998). In this paper, we present the first quantification of the spatio-temporal patterns of periphyton development; and this at high temporal (daily within glacial melt season) and spatial (cm scale) resolutions for an Alpine glacial floodplain system. We test the following hypotheses. First, we hypothesise that periphyton develops preferentially where stable krenal and rhithral water sources flow on terraces. The double condition of water availability and stability allows for longer growth periods because glacial water does not intrude into these channels, and prolonged conditions of water transparency and streambed stability are found simultaneously. Second and in agreement with the literature, we hypothesise a relationship between periphyton development and stability, but we extend the notion of stability to any streambed patch that is stable for long enough to allow for periphyton development. In this sense, we hypothesise that intense braiding likely favours the emergence of braids with more benign conditions (i.e., shallow water and low shear stress) that periphyton may colonize very rapidly. This also extends to braids that have intermittent water supply, and are inundated only at high flows but do not experience substantial hydraulic disturbance. However, this colonization is likely of short duration due to a high probability of disturbance by active reworking of the channel. Finally, we hypothesise that periphyton development at the whole floodplain scale is the net result of the above-mentioned processes and reflects the spatially heterogeneous assemblage of disturbances in the most active portion of the floodplain and of the positive effect of the less destructive non-glacial water sources (e.g., krenal and rhithral) that may drain the most stable portions of the floodplain. This net result eventually defines where ecosystem engineering may occur (see Roncoroni et al., 2019).

2. Methods

2.1. Study site

The Otemma glacial floodplain (Fig. 1, 45°56′04.9″N 7°24′46.1″E) is located in the Val de Bagnes in Southwestern Switzerland. It has formed since the early 2000s in response to very rapid recession of the Otemma glacier (Egli et al., 2021) at an average rate of 50 m per year (Mancini and Lane, 2020). The floodplain, constrained upstream by crystalline bedrock and downstream and laterally by steeper slopes, is approximately 900 m long and 150 m wide. It includes kryal, krenal and rhithral water sources. The floodplain is highly dynamic during the melt-season (Mancini and Lane, 2020) restricting pioneer vegetation and stream periphyton development to surfaces with low rates of morphodynamic activity (Miller and Lane, 2019; Roncoroni et al., 2022; Brandani et al., 2022).

Our dataset is based upon high spatio-temporal resolution optical (i.e. red-green-blue (RGB) band) imagery acquired using a method developed and tested for periphyton mapping (Roncoroni et al., 2022).

2.2. Acquisition of images, ground control points, and Structure-from-Motion photogrammetric processing

We acquired RGB imagery of the floodplain on 52 non-consecutive days from late June to early September 2020. Images were collected with a DJI Phantom 4 Pro quadcopter, which is low cost, allows pre-programmed flight missions and has a camera of sufficient quality for Structure-from-Motion Multiview-Stereo (SfM-MVS) photogrammetric studies (James et al., 2020).

We flew the Uncrewed Aerial Vehicle (UAV) platform early in the morning (from 06 h30 onwards) to avoid extensive inundation of the floodplain, and used the freeware Pix4Dcapture (v. 4.8.0) to manage flight missions and image collection. Following James et al. (2020), we designed the flight missions to produce high precision and quality orthomosaics and Digital Elevation Models (DEMs). Images were collected in grids at 80 m above the ground with the camera looking at nadir (90°) and image overlap of 80 %. Additionally, we included off-nadir center-looking imagery by collecting images in circular missions at 60 m above the ground. We measured the position of 77 Ground Control Points (GCPs) with a differential GPS Trimble R10, with a known and corrected (using the fixed monitoring Swiss Federal Office for Topography provided via SwiPOS©) base station. GCP absolute position was collected in the Swiss coordinate system CH1903+.

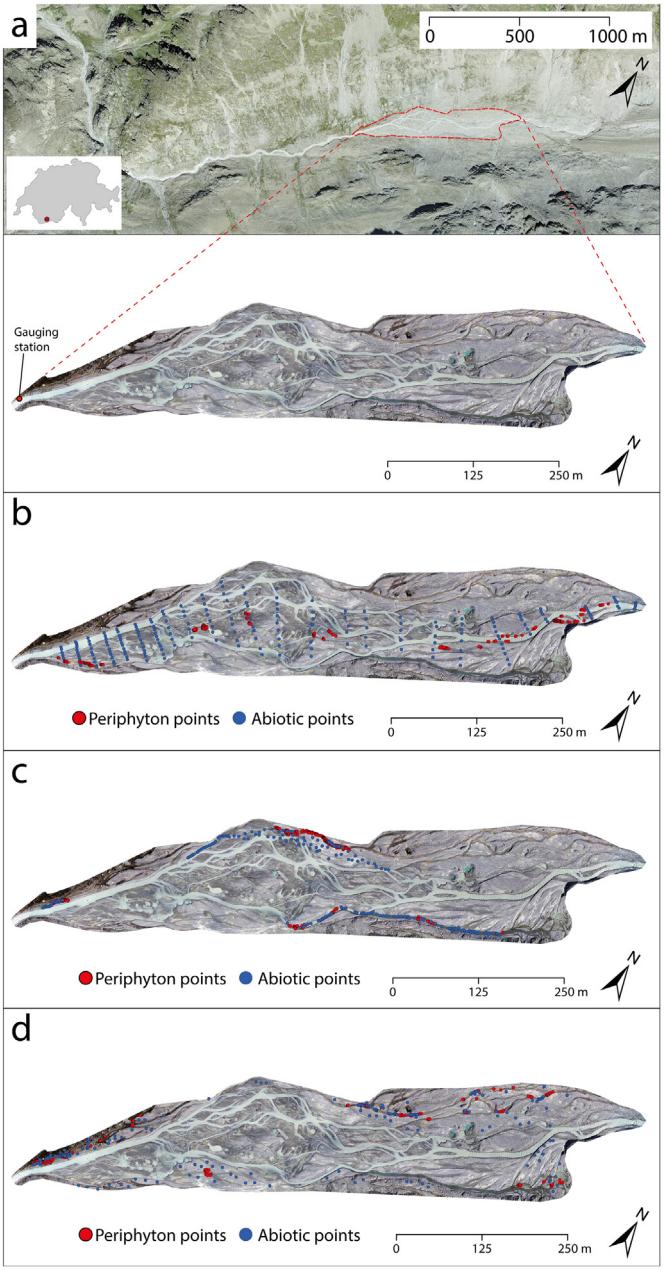

Fig. 1. a) Headwaters of the Dranse de Bagnes (top view; orthomosaic ©*Swisstopo*) and zoom of the study zone (floodplain of the Otemma glacier, bottom view); b) Locations of the sampling points within the active floodplain; c) Locations of the sampling points within the buffer floodplain; d) Locations of the sampling points within the terrace zone.

We undertook the SfM-MVS photogrammetric processing in Agisoft Metashape (v. 1.5.5) and followed the framework of James et al. (2017, 2020) to ensure reliability and replicability within the datasets. To do so, we tested the camera internal parameters and GCP effectiveness in the bundle adjustment to lower the probability of producing datasets with systematic deformations (e.g., doming, datum shift). For the characteristics of our study site, our tests showed that the use of focal length, principal point offset (Cx, Cy), affinity and orthogonality parameters (B1, B2), radial (K1, K2, K3) and decentering (P1, P2) distortions within the bundle adjustment delivered the lowest probability of producing systematic deformations. Furthermore, the tests showed that 52 (68 %) out of 77 GCPs were sufficient to produce high quality 3D re-shaping and scaling of the point clouds (from which DEMs are then interpolated). We then exported DEMs at 20 cm and orthomosaics at 5 cm spatial resolutions. Further details can be found in Roncoroni et al. (2022).

2.3. Periphyton occupation map

We developed date-by-date calibration and validation datasets. Each dataset (i.e., training and validation) consisted of the coordinates of 300 pixels (n = 150 of pure periphyton; n = 150 of un-colonized substrata or turbid water). The pixel selection was based upon visual inspection of our orthomosaics, and this was possible due to the orthomosaic resolutions. Periphyton pixels were chosen to account for the different colour assumed by the periphyton at the time of image acquisition. Following tests (Roncoroni et al., 2022), we segmented each orthomosaic into single visible bands (red, green and blue). We then calculated a visible band ratio, the KANA index (Kawashima and Nakatani, 1998):

$$\mathrm{KANA} = (\mathrm{R}–\mathrm{B})/(\mathrm{R} + \mathrm{B}) \quad (1)$$

where R and B are the intensities of the red and blue bands respectively. The KANA index has the advantage of accounting for the red band that has a beneficial effect in mapping vegetation (Gitelson et al., 2002) and the blue band that has a nearly constant response to chlorophyll-*a* (Kawashima and Nakatani, 1998). Once every orthomosaic was converted into the KANA index, we used the calibration pixels to train date-by-date logistic models. After model validation, we applied the logistic models to map phototrophic periphyton at the floodplain scale (Roncoroni et al., 2022).

We converted the probability maps into binary maps: pixels with a probability <0.5 were classified as not being periphyton whilst pixels with probability >0.5 as being periphyton. A preliminary occupation map, where each pixel corresponds to the days of periphyton occupation (0–80 days), was produced by summing up each binary map after having calculated its own time-lag compared to t_{n-1} and t_{n+1} (i.e. time-lag: $[(T - T_{n-1})/2 + (T_{n+1} - T)/2]$). We then assessed the noise in the occupation map by undertaking a runs test and excluded pixels with a probability <95 % ($p_{value} < 0.05$) of reflecting true periphyton dynamics (Roncoroni et al., 2022). Orthomosaic segmentations, visible band ratio calculations, logistic regressions, occupation maps and runs test were performed in Matlab (R2018a).

2.4. Submersion maps and geographical area segmentation

In a GIS environment (ArcMap, v. 10.5.1), we digitized the edges of the channels visible in each dataset (i.e., date) to allow determination of inundation extent at low discharge. Stacking each dataset allowed us to determine the number of days that each pixel in the floodplain was permanently inundated at low flow. Furthermore, this allowed calculation of braiding characteristics.

Following the channel segmentation of Ward et al. (1998), we then defined three geographical zones with distinctive hydrological properties. The first was defined as the active zone that was delimited by the maximum extent of glacially-fed water, but excluding zones with hillslope or groundwater derived clear water that was intermittently flooded by glacial-fed water. Within the active zone, as this was a braiding system, there was always the potential for inundation at high flow or morphodynamic change. However, there were areas in the active zone that during our study were morphologically more stable and other areas more dynamic. The second zone was one that had no incursion of glacier-derived water during the study period. This was primarily but not exclusively on low altitude (0.5 to 1 m) terraces and so we call this the terrace zone. The third zone was the buffer zone that effectively marked the interface between the active and terrace zones and included areas that contained intermittently clear and glacially-fed water.

To test for significant differences within the geographical areas of the floodplain (i.e., active, buffer, and stable), we finally performed a non-parametric Kruskal-Wallis.

2.5. Discharge time-series

At the downstream end of the floodplain (Fig. 1), a gauging station site composed of (i) a Campbell CR200 datalogger with a CS451 pressure transducer and (ii) a Keller DCX-22AA-CTD logger and pressure transducer was installed. Continuous river stage measures were carried out during summer 2020, and here we use the data from June 26th to September 13th. Between July 19th and September 9th 2020, 21 discharge (m^3s^{-1}) measurements were derived from dye or salt (in the case of discharge lower than 0.5 m^3s^{-1}) tracings. These spot measurements were used to construct a stage-discharge relationship that was in turn used to provide a discharge time-series. The full details of these methods are provided in Müller et al. (2022).

2.6. Braiding index measures

Braiding indices were calculated using a channel count index that determines the number of channels (n_c) in cross-sections (i) perpendicular to the main valley direction (Hong and Davies, 1979; Mosley, 1982; Ashmore, 1988; Chew and Ashmore, 2001; Egozi and Ashmore, 2008). We do not apply the Howard et al. (1970) requirement that cross-sections should be sufficiently far apart that no secondary channel is included in more than one cross-section. For n_s cross-sections, this gives a channel count braiding index (B_c) defined as

$$B_c = \frac{\sum_i^{n_s} n_c^i}{n_s} \quad (2)$$

2.7. Instability maps

We used the DEMs to produce an instability map that illustrates the number of days of instability (i.e., disturbances) in each pixel of the study site. This method was proposed by Lane and Richards (1997) and more recently by Bakker et al. (2019) to understand river-bed age, i.e. the time since the last stream reworking.

First, we calculated a set ($n = 51$) of limits of detection (LoD) which defines the magnitude of vertical change between two DEMs needed for 95 % confidence that the change is statistically significant given noise in the DEM data (see supplementary material SM1). This is a standard practice in geomorphic change detection (Brasington et al., 2000, 2003; Lane et al., 2003; Milan et al., 2011; Bakker et al., 2019; Roncoroni and Lane, 2019; Mancini and Lane, 2020). In our case, we calculated a moving LOD (i.e., pairs of days, June 26th versus June 27th, June 27th versus June 28th) between any two DEMs at times T *and* $T + 1$ assuming that DEM errors are Gaussian and pairwise independent (in time);

$$LoD_{T,T+1} = \pm t\left[\sigma_T^2 + \sigma_{T+1}^2\right]^{0.5} \quad (3)$$

where t is the confidence interval (here 95 %, so $t = 1.96$), σ_T is the standard deviation of errors in DEM at time T.

Second, we calculated DEMs of Difference (DoD) by subtracting DEMs for each LoD to produce a set of DoDs (Brasington et al., 2000, 2003; Lane et al., 2003) and applied the associated LoD to identify significant changes.

Third, the thresholded DoDs were converted into binary change maps, in which we attributed 0 (i.e., stable) to elevation changes within the ± LoD range and 1 (i.e., change) to changes exceeding the ±LoD range. We then stuck the binary change maps by applying the time-lag scalar (i.e. time-lag: $[(T - T_{n-1})/2 + (T_{n+1} - T)/2]$) used in Sections 2.3 and 2.4, obtaining an instability map (0–80 days).

2.8. Periphyton point sampling and parameter extraction

On the occupation map and for each floodplain geographical area (i.e., stable, buffer, and active) we selected 400 periphyton and 200 non-periphyton (e.g., sediments, water) points (see supplementary material SM2). The point coordinates were used to extract: (i) the percentage of time the point was occupied by periphyton; (ii) the percentage of time the point was unstable; (iii) the mean change in elevation from the closest glacial channel; (iv) the mean distance from the closest glacial channel; and (v) the percentage of time the point was submerged.

For the three habitats and on a date-by-date basis, we also extracted the daily periphyton presence/absence (0–1) from the periphyton binary maps and the submerged/dry (0–1) from the daily inundation maps.

Finally, for a general comparison of the three habitats, we also extracted the total number of pixels with at least one day of periphyton occupation.

3. Results

3.1. Occupation, submergence and instability

Within the active floodplain boundaries (Fig. 2a), periphyton occupations were low (Fig. 3a; supplementary material SM2), infrequent (Fig. 3d), and spatially localized (Fig. 2a). Meanwhile, 70.2 % of the active zone was submerged by glacial water for at least one day during summer 2020 (supplementary material SM3), with submergence rates generally high (Fig. 3b), and a strongly braided and dynamic stream system (Fig. 2b). Unstable surfaces were widespread across the active floodplain (Fig. 2c), and 61.8 % of this area was reworked for at least one day during the summer (supplementary material SM3), although instability rates were rather low (Fig. 3c; supplementary material SM2).

Periphyton occupations in the buffer zone (Fig. 2a) were higher than in the active zone (Fig. 3a, d; supplementary material SM2), with buffer surfaces occupied by periphyton 30.9 % of time in average. 78.5 % of the buffer surface was submerged (either by glacial or clear water) for at least one day during the study period, with 75 % of this zone submerged for at least 1.9 % of the time (Fig. 3b; supplementary material SM3). The higher submergence rates as compared to the active zone reflected the constant, yet stable, contribution of the clear water fed channels draining the buffer zone. Although occupations were high on average, the buffer zone was often unstable (Figs. 2c, 3c; supplementary material SM2) and 73.7 % of the buffer zone experienced at least one disturbance episode during the study period.

The highest occupations were found in the terrace zone (Figs. 2a, 3a, d), with periphyton occupying the streambeds 38.8 % of the time in average (supplementary material SM2). Periphyton locations were tied to channel locations, which covered 10 % of the terrace zones (supplementary material SM3). To put this into context, the terrace zones accounted for 72 % (713 m^2) of the periphyton coverage of the entire floodplain. The terrace zone was thus characterized by dry conditions (Fig. 3b), but submerged areas when present were generally stable through time (Figs. 2c, 3c; supplementary material SM2) and were not impacted by major disturbances (e.g. hillslope-originating mass movements) during the study period.

Finally, Kruskal-Wallis results showed significant differences among the geographical areas in response of occupation ($p < 0.001$), submergence ($p < 0.001$), and instability ($p < 0.001$). These results suggested that zonation was appropriate and distinct biofilm habitats existed within the floodplain.

3.2. Relationship between periphyton development and the physical habitat

Occupation was low (<20 % of the time) within the sampling point population of the active floodplain (Fig. 4). In this zone, periphyton were commonly found in relatively stable surfaces that experienced stream reworking for <40 % of the melt-season period (Fig. 4a; supplementary material SM4). Nevertheless, the majority of the streambed occupied by periphyton occurred in areas that were unstable for <20 % of the time (supplementary material SM4). Not surprisingly, instability rates tended to increase submergence by glacially-fed water (Fig. 4a). However, submergence of 40 to 70 % was also found to be beneficial for periphyton, but only when instability was simultaneously low (Fig. 4b; supplementary material SM4).

The sampling points had relatively small elevation differences (−0.3–1 m), but were quite spread laterally (0–35 m) compared to the

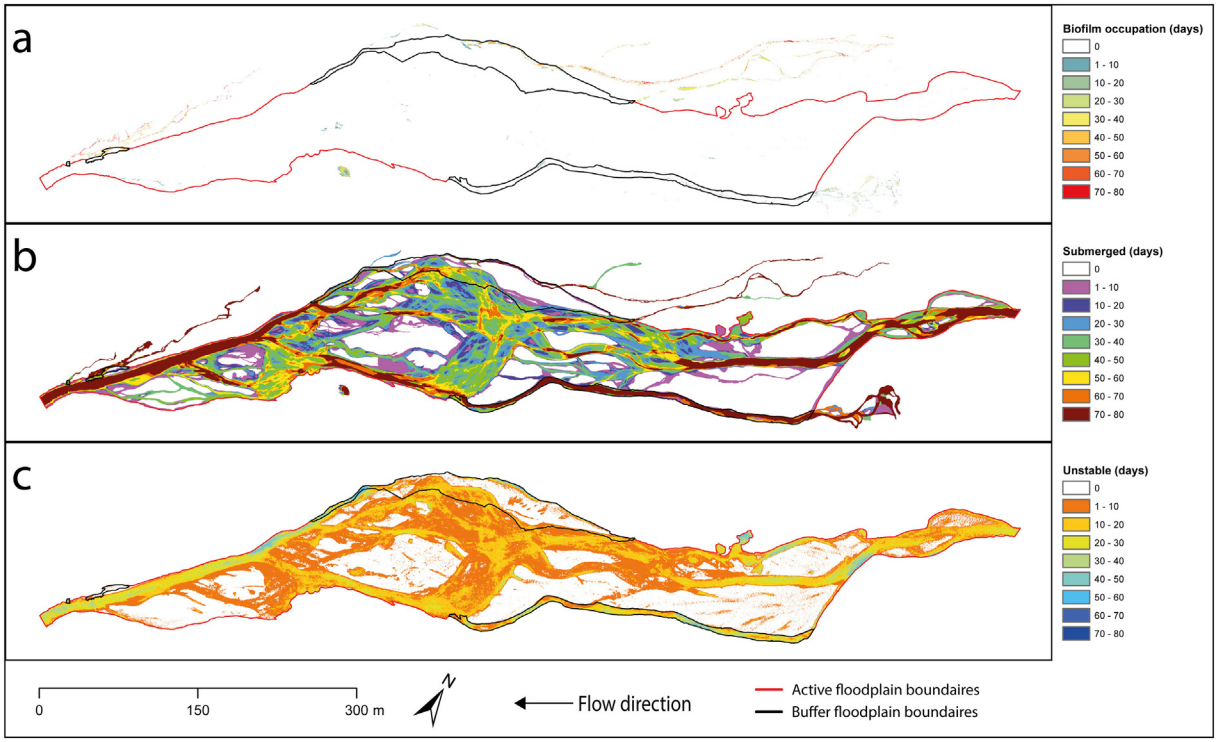

Fig. 2. a) Periphyton occupation in number of days (see Roncoroni et al., 2022); b) Submergence in number of days; c) Instability in number of days. The interior of the black bounding boxes is the buffer zone; of the red bounding box the active zone (except for the buffer zone); and outside the red/black boxes the terrace zone.

closest glacial channel (Fig. 4c). However, most of the periphyton points had positive mean elevation differences (0–0.1 m) but relatively little lateral distances compared to the closest glacial channel (0–5 m; Fig. 4c). Periphyton likely used marginal channels that were cut off from the main active stream system and became dry at some point during the melt-season. On the other hand, unoccupied points (i.e., white dots with black outlines in Fig. 4c) tended to be located at greater elevation differences (above 0.1 m) or greater distances (from 10 m), which suggest drier conditions due to the greater disconnection from glacial water.

In the buffer zone, unstable points typically had high submergence rates (Fig. 5a). However, the highest submergence rates did not always lead to the highest instabilities (Fig. 5b). Periphyton presence followed this trend and periphyton preferentially used the streambed patches that were more stable and also the most submerged (Fig. 5ab; supplementary material SM5), although cases in which periphyton developed on more unstable or drier surfaces existed.

The mean altitude differences between the sampling points and the closest glacial channels (Fig. 5c) showed a clear dichotomy in the buffer floodplain. Unoccupied or low occupation points used lower altitudes (i.e., smaller elevation differences) while medium to high occupation points were found at greater altitudes compared to the closest glacial channel. This clear dichotomy was likely the result of glacial water flooding into the buffer zone, with lower surfaces being flooded more easily (so low or no occupations) and higher surfaces being rarely flooded (so medium or high occupations). Laterally, unoccupied patches were typically found closer to the glacial channels or far from them. In the first case, short lateral distances, coupled with small elevation differences, made glacial water intrusion easier and disturbances more frequent; in the second case greater lateral distances made glacial intrusion more rare resulting in drier conditions.

Glacial water intrusion in the buffer zone had a clear negative impact on periphyton occupation (Fig. 6; supplementary material SM6). In fact, the highest occupations as well as the highest number of occupied points were found on surfaces that were rarely inundated by glacial water, but that were submerged by clear water most of the time. On the contrary, only a few periphyton points were found on surfaces that were also often flooded by glacial water.

Access to water was crucial on the terraces, and most of the periphyton points were found in channels with submergence rates >80 % (Fig. 7a; supplementary material SM7). Those locations were identified across all elevation ranges and across all distances from the nearest glacial stream. On the other hand, unoccupied points were mostly found on dry surfaces (supplementary material SM7), that also had high altitudes compared to or were far from the closest glacial channel (Fig. 7b), so that the floodplain water table was likely too low to provide water to the surface and sustain periphyton accrual. Compared to the active and buffer floodplains, our results suggest that periphyton development was only limited by water availability.

3.3. Temporally resolved periphyton physical habitat

We quantified the temporal evolution of periphyton presence/absence coupled with inundation data and in relation to the daily low/high discharge and braiding index over the entire 2020 melt-season (Fig. 8).

Periphyton in the terrace zone (Fig. 8a) had typically long periods of growth and survival, and some channel sections were already colonized before the 26th of June (or Julian Day, JD 178). It appeared that several periphyton locations (0–150) disappeared around the end of July (from JD 210); but returned from JD 220. Other periphyton locations (200–400) behaved in a similar way, but for different dates. There were streambed patches with periphyton that were not submerged by clear water during the drone surveys, suggesting daily fluctuations of the tributary water levels and the capability of periphyton to survive short periods of drought. It appeared that the terrace zones were not influenced by variations in the glacial daily low/high discharge (Fig. 8d) even though channel desiccation events did occur around JD 223 when ice-melt slowed and discharge began to fall. This could potentially be traced to the progressive exhaustion of ground-fed and high-altitude snowmelt water sources, which correlates with declining glacier melt.

The buffer zone (Fig. 8b) was more complex compared to the terrace zone. Periphyton locations 0 to 25 lasted for about 60 days. Periphyton

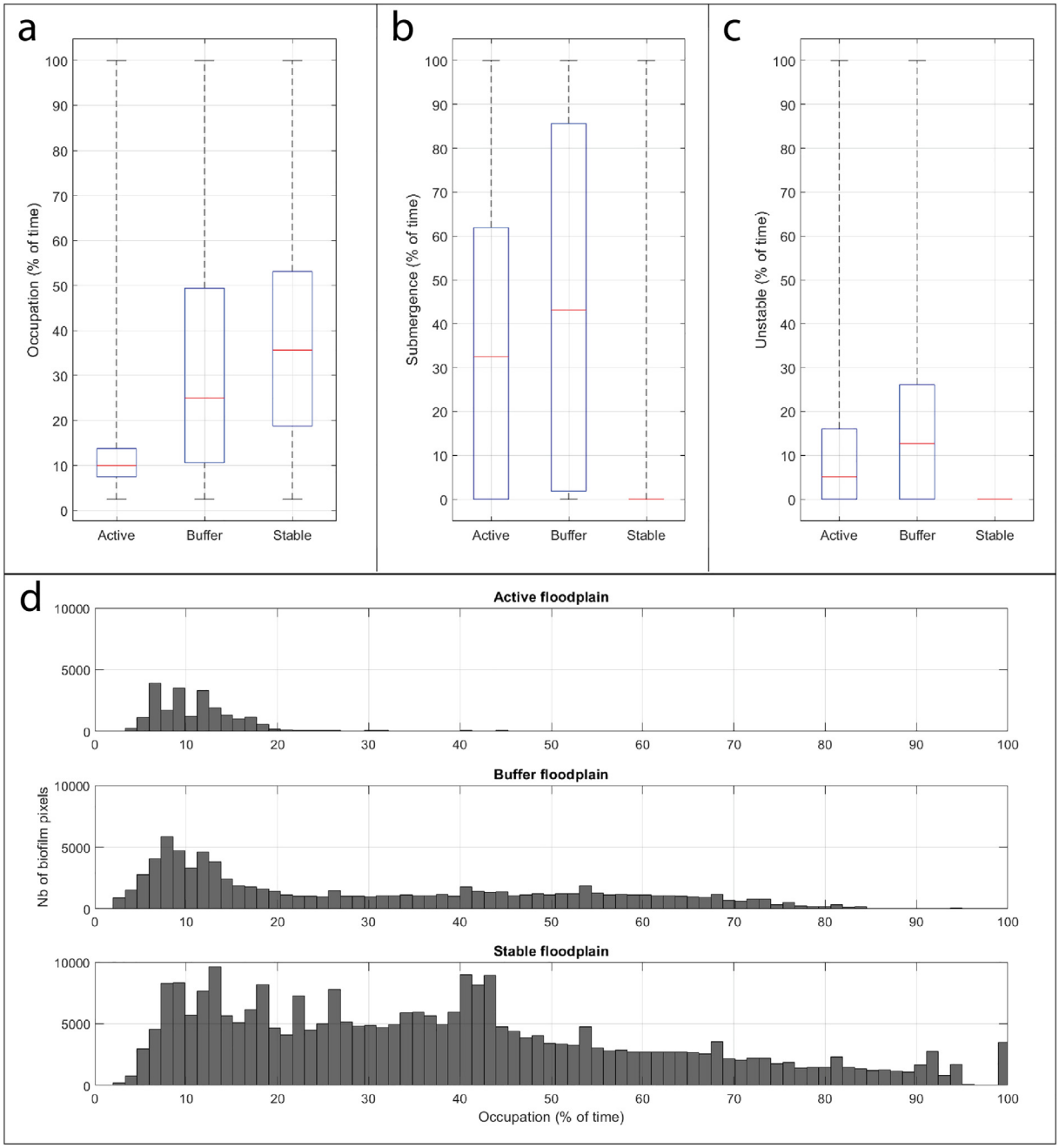

Fig. 3. Comparison of a) the periphyton occupations (in % of time, 80 days is 100 %) between the geographical areas of the floodplain; b) the submergence (in % of time); and c) the instability (n % of time). d) Frequency of periphyton occupation (in % of time) for active, buffer, and stable zones. In 3a, 3b and 3c the whiskers define the data range and the box the 25 %, 50 % and 75 % percentiles.

were then removed, notably associated with the intrusion of glacier-originating water around JD 238. Locations 25 to 51 partially disappeared around JD 217 due to desiccation of the channel. Locations 80 to 360 suggested some disturbance by glacial water with the sudden disappearance of most of the periphyton locations around JD 186 and JD 188. Though the locations were mapped as being clear water during the morning drone survey, we noted that glacial water flooded those surfaces during the daily peak flow events (Fig. 8d). Locations 80 to 360 began to recover, notably from JD 210 onwards.

The active zone (Fig. 8c) suggested a strong linkage between periphyton presence, glacial water and stream morphodynamics. At the beginning of the survey season (JD 178-190), discharge was high, so was the inundation extent, and braiding was minimal, resulting in wider channels with harsh conditions for periphyton. The majority of periphyton locations developed between JD 190 and JD 220, and all those locations shared the same patterns of accrual and removal by glacial water. Periphyton accrual usually happened after a drop in discharge whilst removal often happened after a discharge increment (Fig. 8d). This gives the appearance of short windows of opportunity. During this period of development, the braiding intensity and the bar numbers were at their maximum (Figure 8ef), whilst the mean bar areas and the average distances of the bars from the glacial channels at their lowest (Figure 8gh). In this sense, the likelihood of having smaller, shallower, less harsh anabranches that supported periphyton development was higher. We also found periphyton that were not submerged during our low flow drone surveys (e.g., JD 202-225, Fig. 8c), suggesting that periphyton were inundated at higher flows within the same day to the extent needed to sustain their development (Fig. 8d), but such water was less destructive. Later in the season, from JD 220 onwards, the glacial

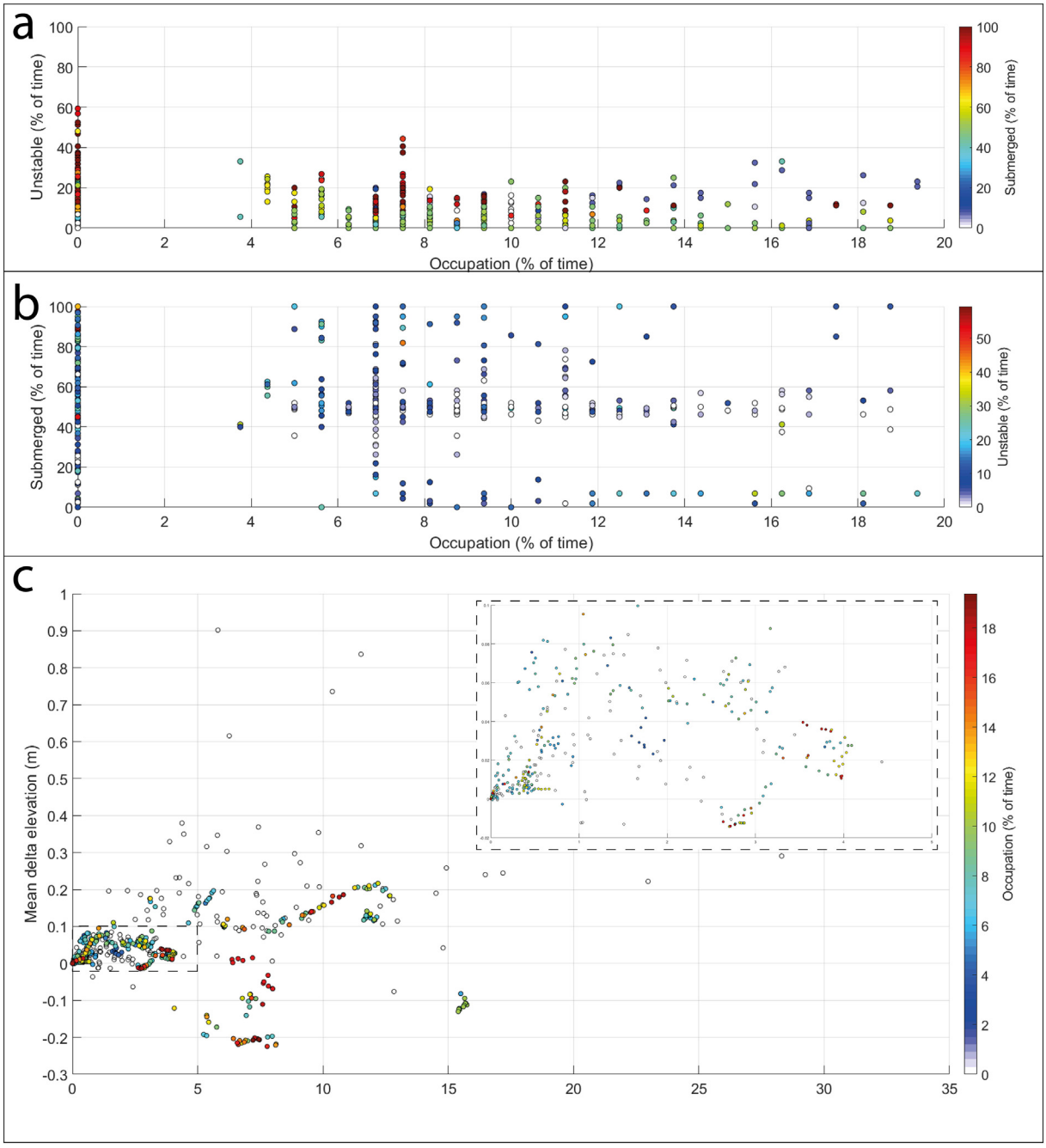

Fig. 4. Relationships between a) instability, occupation and submergence, and b) submergence, occupation and instability for the active floodplain sampling points. c) Seasonal mean elevation difference and distance from the closest glacial channel.

stream system started to shrink (Fig. 8h) turning the previously occupied channels dry and canalizing the bulk of melt-water in a smaller number of braids (Fig. 8e). Periphyton development in the active zone stopped during this period.

4. Discussion

4.1. Physical environment and periphyton habitat

The physical environment of glacial floodplains is dynamic in summer (Marren, 2005; Heckmann et al., 2016; Bakker et al., 2019), limiting periphyton accrual (Milner and Petts, 1994; Uehlinger et al., 1998, 2002, 2010; Battin et al., 2004; Boix Canadell et al., 2021). Our results support these findings, but also highlight the spatiotemporal heterogeneity of hydraulic-related disturbances and the presence of suitable periphyton habitats beyond tributaries (i.e., krenal and rhithral) and terrace tributaries during the melt-season in summer.

Recently-deglaciated floodplains are drained by various water sources including kryal, krenal and rhithral (Malard et al., 1999; Ward et al., 1999) and shaped by different hydro-geomorphic features including stream braiding (Maizels, 2002; Marren, 2005) and terraces (Germanoski and Schumm, 1993; Marren, 2002; Marren and Toomath, 2013, 2014; Roussel et al., 2018). Accounting for these different hydrological and hydro-geomorphic features is indeed important when studying the ecological functioning of glacial floodplains. We segmented the floodplain of Otemma into three geographical zones and showed that these each had distinctive periphyton development patterns (Fig. 2a, Fig. 8) which can be mapped onto both inundation characteristics (Fig. 2b) and river instability (Fig. 2c).

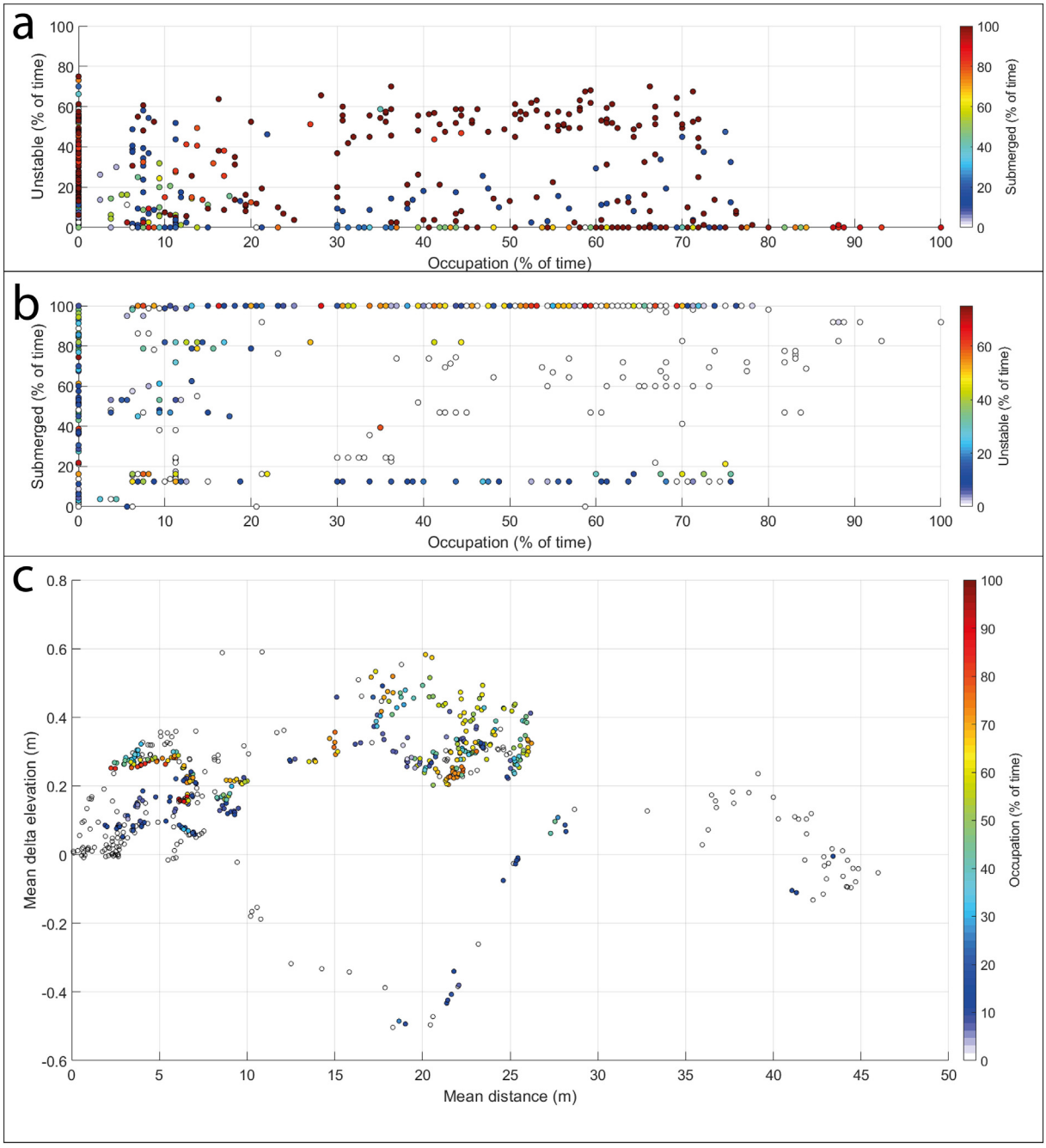

Fig. 5. Relationships between a) instability, occupation and submergence, and b) submergence, occupation and instability for the buffer floodplain sampling points. c) Seasonal mean elevation difference and distance from the closest glacial channel.

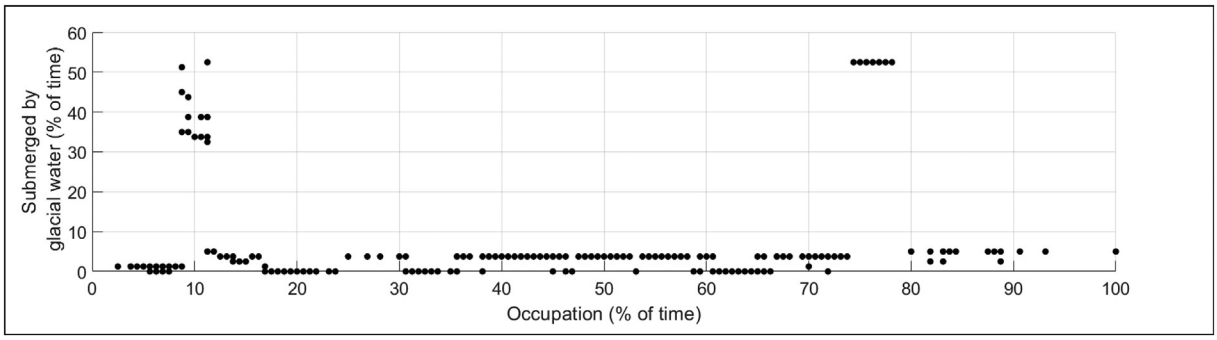

Fig. 6. Influence of glacial water on periphyton occupation within the buffer zone.

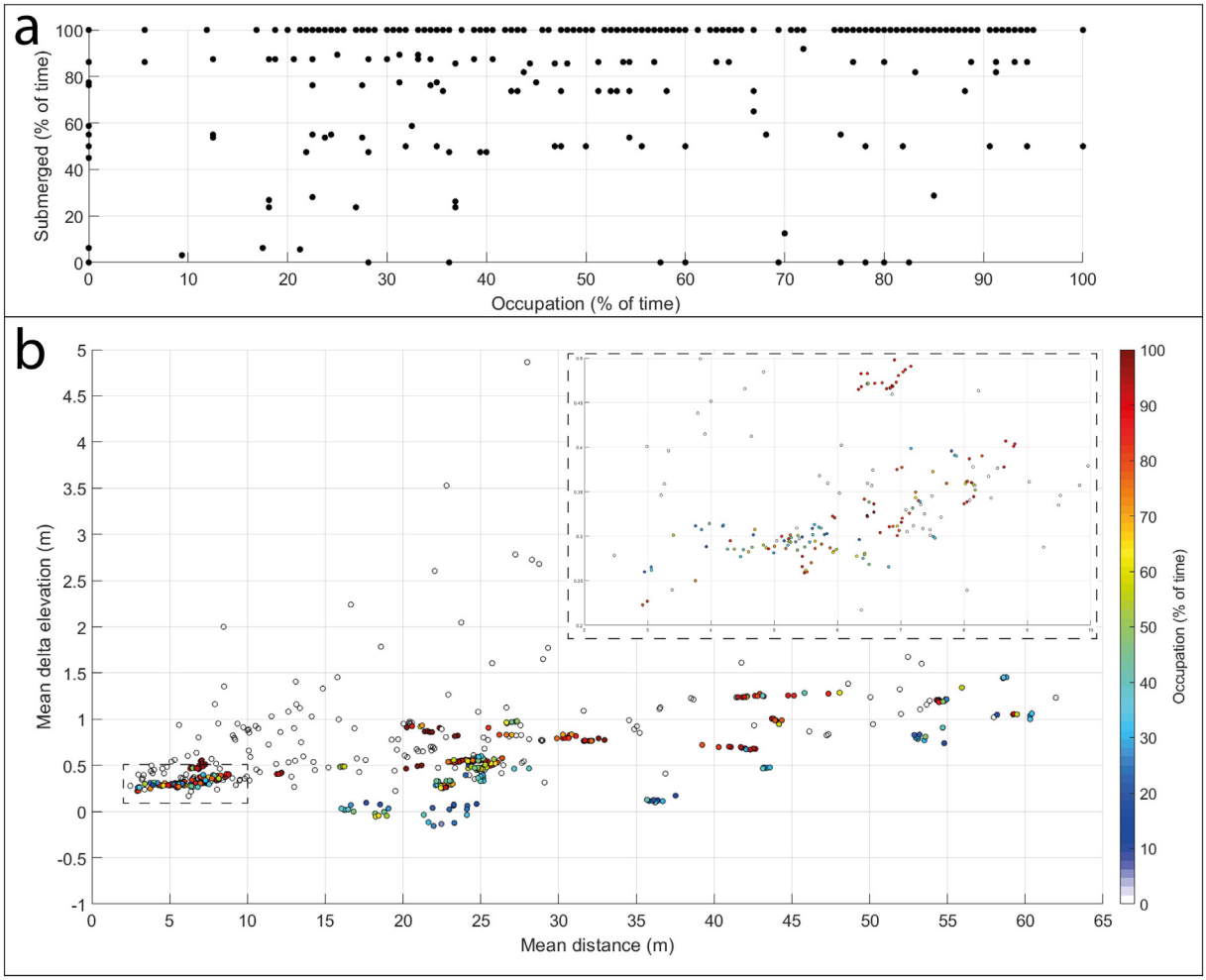

Fig. 7. Relationships between a) submergence, occupation and instability for the terrace zone sampling points; b) seasonal mean elevation difference and distance from the closest glacial channel.

The importance of access to krenal and rhithral water was clear in our study site with periphyton on the stable terraces concentrated in channels constantly fed by adjacent hillslopes (hypothesis 1). Equally, despite extensive inundation in the active zone, this water was invariably turbid and periphyton only developed significantly where water was very shallow or in braids inundated only at high flows (hypothesis 2). In the active zone, where rates of floodplain reworking were highest (Fig. 2c), periphyton were ephemeral (Fig. 8c) with low occupation rates (Fig. 3d), appearing in short windows when conditions were stable (hypothesis 2). We confirmed a link between these processes and the intensity of river braiding (Fig. 8) (hypothesis 2) and in the active zone, windows of opportunity appeared when the river was most braided, so reducing the average distance to (glacial) water and increasing the likelihood that flows were shallow. These windows of opportunity were only of short duration (hypothesis 2; Fig. 8c) because of the intensity of disturbance of the active zone (Fig. 2c).

Within our study site, we characterize three zones with distinct periphyton dynamics. In the active zone, periphyton accrual is limited in space and time (Figs. 2a, 3ad, 4 and 8c), and periphyton develop in short windows of opportunity linked to three processes: (i) access to glacial water; (ii) periods of stability; and hence (iii) stream morphodynamics. In the summer of 2020, access to glacial water passed through what appears to be an optimal window (Fig. 8). At first, to JD190, inundation by glacial water at low flow was extensive, resulting in channels with harsh conditions due to the high amount of glacially-fed water distributed in a limited number of channels (Fig. 8e). From JD 190 onwards, draining of the floodplain caused a rapid increase in bar numbers and area (Fig. 8fg), forming channels that were hydraulically less harsh (Ashmore, 1988; Ashmore et al., 2011), with increased streambed stability and likely shallower (Warburton and Davies, 1994) such that the phototrophically-active radiation could reach the channel bottom. Our results also show that periphyton developed on surfaces that were dry during low flows (Fig. 8c), but likely submerged by water during high flows (Fig. 8d) such that survival was guaranteed. In this sense, research has demonstrated, notably in Antarctica, that benthic periphyton can survive extended drought periods (McKnight et al., 2007) and remain photosynthetically-active in hours when re-submerged (Hawes and Howard-Williams, 1998). Later in the season (from JD 220), those periphyton areas were reworked such that periphyton eventually were removed. From JD 220 onwards, the river incised, braiding index and the number of bars fell (Fig. 8ef); these areas became almost permanently dry (Fig. 8c), and progressively more distant from glacial water (Fig. 8h). Periphyton development ceased even though stability increases during this period. Thus, periphyton presence in the active zone is related to windows of opportunity in the active zone and associated with areas that are periodically and locally less harsh or intermittent and largely morphodynamically stable. As inundation tends towards being permanent so it is more likely to be deeper and faster flowing, slowing periphyton development and increasing the probability of its removal. The result is that there are zones present in the active floodplain that can support periphyton provided that there is some but not too much glacial water supply, but these are spatially-restricted and also dynamic as river morphodynamics can change locally how harsh the water is (water depth; bed shear stress) as well as the ease of access to that water. In the case reported here, a seasonal shift towards less braiding (Fig. 8e) eventually increased the average distance from channels containing glacial water and for sites

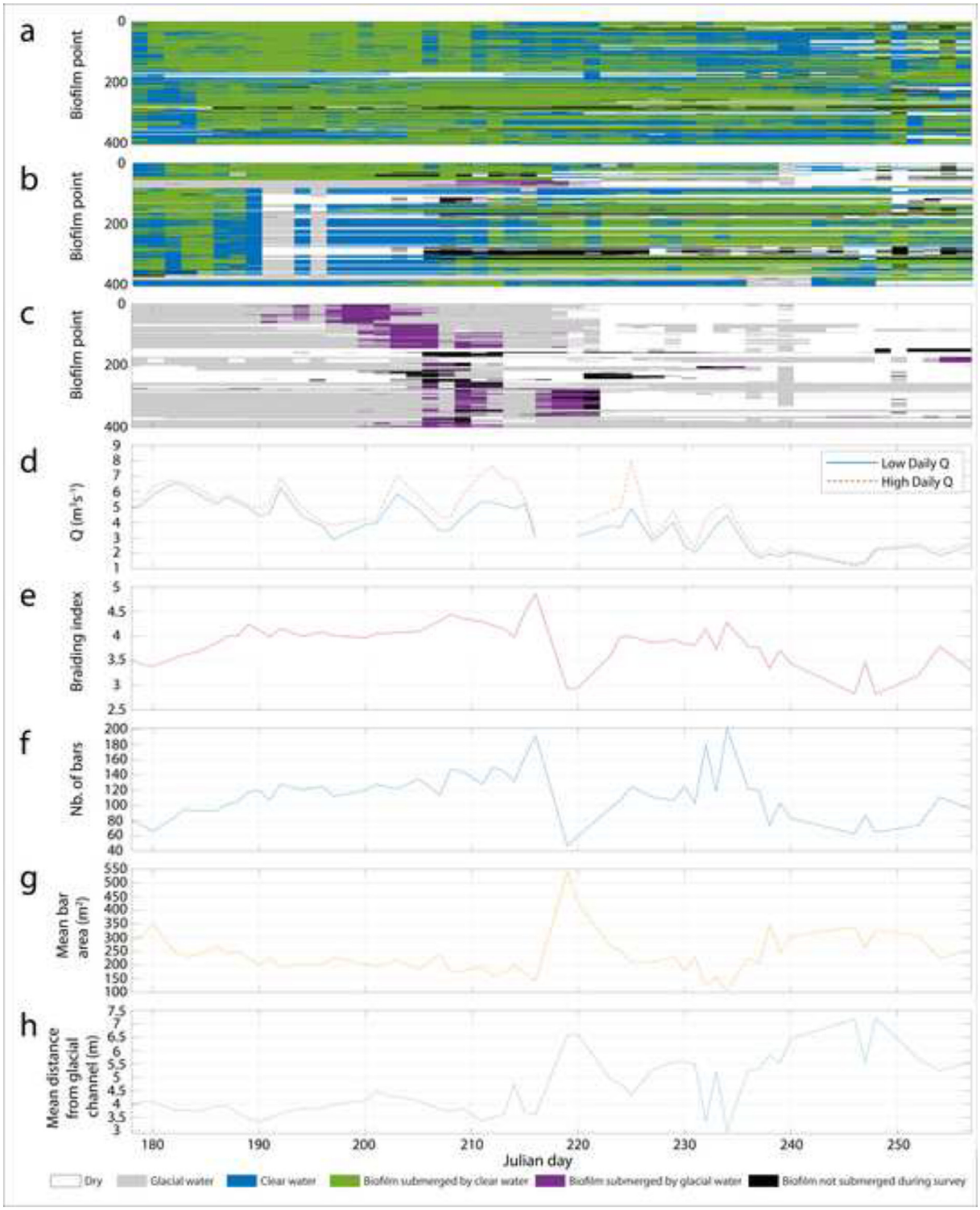

Fig. 8. Temporally resolved peripyhton physical habitat within a) terrace, b) buffer and c) active zones; d) Daily low and high Qs (m^3s^{-1}); e) Braiding index; f) Number of bars; g) Mean bar area (m^2); and h) Average distance from bars to glacial channels (m).

that were not permanently inundated periphyton presence largely ended (Fig. 8c). The linkage to braiding implies that wider exogenic drivers of braiding intensity (notably the ratio glacier sediment supply to sediment transport capacity, a function of glacier melt rate) will in turn drive periphyton dynamics in the active zone.

The buffer zone represents one where there is progressively less glacial water intrusion but there is permanent non-glacial water supply. Unlike in the active channel, the permanent availability of clear water means that periphyton presence can approach being perennial (Fig. 3b) although not throughout this zone. In the buffer zone, glacial water may intrude clear water channels, periphyton are impacted and their survival reduced (Fig. 6) and this is likely due to sudden but sometimes short-lived changes in habitat conditions (i.e., from clear to glacial water) and increased streambed instability (Figure 5ab). However, periphyton can recover (Fig. 8b) within a relatively short time (Battin et al., 2003) if clear water flow resumes. Higher elevations compared to the closest glacial channels

(Fig. 5c) clearly host higher greater periphyton occupation in this zone because glacial water intrusion is less common, and probably less destructive. As these zones are more likely to have water, they may become hotspots for eventual primary vegetation succession as long as the magnitude and frequency of disturbance by the glacial stream remains low.

The terrace zone is unimpacted by glacial water. Terraces are common in glacial floodplains (Marren, 2002, 2005; Marren and Toomath, 2013, 2014; Roussel et al., 2018) due to systematic shifts in the balance between glacial sediment supply and sediment transport capacity. Terraces commonly form when capacity exceeds supply and this matters in terms of stability. The disconnection (Fig. 7b) from the glacial stream leads to a stable habitat that is never (i.e., the case of summer 2020) or very rarely inundated by glacial water. In theory, the lack of access to glacial water becomes a limit and it makes periphyton colonization in this zone highly-dependent on snow-melt or groundwater-fed streams (Malard et al., 1999; Ward et al., 1999). Such water is substantially less harsh and periphyton development is enhanced due to water transparency and overall hydrological, hydraulic and thermal stability (Boix Canadell et al., 2021); but it is also spatially restricted leading to periphyton development that is localized (Fig. 2a) to the streams that cross this zone. In such areas, we find the highest rates of periphyton coverage (Fig. 3ad) with the highest occupation days (Fig. 2a; Roncoroni et al., 2022) compared to the buffer and active zones. Our results (Fig. 8a) also suggest a periodic renewal of periphyton mats, followed by rapid re-colonization of the streambed. That said, there are other potential disturbances to periphyton habitats in this zone. Progressive snow-melt decline, which may also cause a decline in shallow groundwater if it is also snow-melt fed, causes desiccation events to become more common from August onwards (Fig. 8a), tracking the contraction of the stream system at the end of the melt-season (Malard et al., 1999). Roncoroni et al. (2022) found that the terraces of the Otemma glacier floodplain were almost dry during late autumn and periphyton were restricted to the active zone where disturbance had reduced (i.e., window of opportunity; Uehlinger et al., 2002, 2010) and glacial water had much lower suspended sediment concentrations and so was much less harsh.

4.2. Implications for ecosystem engineering

Our results further demonstrate the strong control of the physical habitat template on periphyton accrual, survival and removal. Water accessibility is central in supporting periphyton development (Rydgren et al., 2014), but large amounts of water lead to high shear stresses, notably from ice-melt, and so can become destructive. In this sense, the active zone has the highest annual water availability, but this water provides harsh and unstable conditions. Periods between two disturbances is often so short that periphyton cannot develop or reach a state of maturity (Thom et al., 2015). The negative effect of glacial water is accentuated in the buffer zone where more generalist periphyton are likely to develop. Glacial water intrusion in clear water channels results in sudden habitat changes that, depending on the length of the events, could lead to periphyton removal. Our results suggest that glacial water – and hence the associated high shear stresses, bed and suspended loads – shapes the ecological functioning of glacial floodplains by creating a disturbance-dominated regime that results in an ephemeralisation of the periphyton habitat. Active and buffer zones should indeed be regarded as ephemeral habitats, where periphyton may only develop in specific, short windows and zones of opportunity within the melt-season (hypothesis 3).

On the other hand, tributaries on disconnected terraces that are rarely if never inundated by glacial water should be considered as perennial habitats during the melt-season (hypothesis 3) due to higher algal biomass (Brandani et al., 2022) and long survival periods (Roncoroni et al., 2022). These perennial habitats are stable, drained by clear water (Boix Canadell et al., 2021) and are also enriched in dissolved organic matter (Brandani et al., 2022).

Different studies consider periphyton as ecosystem engineering agents (Gerbersdorf et al., 2008, 2009), even in glacial floodplains (Miller and Lane, 2019; Roncoroni et al., 2019). In glacial floodplains, benthic periphyton are thought to fertilize the nutrient-deprived glaciogenic sediments, maintain the water at the surface by creating an impermeable layer at the streambed surface and, to a smaller extent, stabilize streambed sediments (Miller and Lane, 2019; Roncoroni et al., 2019). Such engineering effects are supposed to promote primary succession and to explain patterns of succession that do not follow the chronosequences of Matthews (1992). Our results suggest that ecosystem engineering likely only occurs in perennial habitats, which support long-term periphyton during the melt-season, also when vegetation can grow at such high altitudes. On the contrary, ephemeral habitats might hold the highest cumulative biomasses (especially during windows of opportunity; Uehlinger et al., 2002, 2010), but the positive feedbacks associated with periphyton growth are likely to reset on periodic bases without influencing positively vegetation development over the long-term.

5. Conclusions

In this paper, we decrypted the periphyton physical habitat in a recently deglaciated floodplain; and we did this at high temporal and spatial resolutions. We formulated three hypotheses: (i) the simultaneous presence of krenal and rhithral channels over terraces favours the development of periphyton in those zones; (ii) intense stream braiding creates short windows of opportunity; and (iii) periphyton development at the floodplain scale is the net result of the above-mentioned hypothesis and this result matters in terms of ecosystem engineering.

In agreement with the literature (Uehlinger et al., 1998; Ward et al., 1998), we highlighted the importance of krenal and rhithral channels as being hot spots for periphyton but we also demonstrated the importance of channel location. However, krenal and rhithral channels are hot spots only if they flow over terraces. If such channels flow at lower floodplain elevations, they are prone to be inundated by glacial water (i.e., the buffer zone) resulting in harmful effects for periphyton. We also demonstrated that stream morphodynamics (i.e., braiding) have the potential to create zones of ephemeral stability. We demonstrated that when braiding intensity is high, some braids become less harsh so that periphyton may rapidly develop. Equally, we demonstrated that such braids are rapidly cut off by stream dynamics, resulting in periodic periphyton reset. Finally, our results suggest that systematic variation in periphyton presence/absence is strongest laterally rather than longitudinally, and the role of periphyton in driving ecosystem succession following deglaciation is likely concentrated in hotspots where access to water is associated with non-glacial and thus non-harsh conditions, itself related to the heterogeneous assemblage of disturbances in space and time.

Although we find glacial floodplains with similar stream morphodynamics throughout the Alps, and beyond, our results are contextualised to a single system, the Otemma floodplain. We acknowledge this, and we highlight that a more comprehensive understanding of the periphyton physical habitat of recently deglaciated floodplains must require new studies in floodplains with different characteristics (e.g., slope, glacial extent, orientation, discharge, etc.).

Funding information

This study was supported by Swiss National Science Foundation Sinergia grant CRSII5_180241 *ENSEMBLE* awarded to T. J. Battin, S. N. Lane, M. Lever and P. Wilmes.

Credit authorship contribution statement

M.R., T.J.B. and S.N.L. conceived the study; M.R., D.M., F.M., T.M., M.G., M.C., B.O., and F.L. collected and processed the data; all authors contributed to the writing of this paper.

Data availability

Data availability: orthomosaics are available at doi.org/10.5281/zenodo.7514935; periphyton maps are available at doi.org/10.5281/

zenodo.6598305; discharge data available at doi.org/10.5281/zenodo.6202732.

Declaration of competing interest

The authors declare that they have no known competing financial interests or personal relationships that could have appeared to influence the work reported in this paper.

Acknowledgements

We would like to acknowledge Associate Editor Dr. Fernando Pacheco, and two anonymous reviewers for the critical but constructive comments provided on earlier version of this article. We also acknowledge the people that helped us in collecting the UAV imagery during summer 2020: Adrijan Selitaj, Margaux Hoffman, Alissa Pott, Lara Mercier, Gwendoline Perritaz, Isabel Herr, Pierre Hauptmann, Valentine Grünwald and Valentin Cina-Colman.

Appendix A. Supplementary data

Supplementary data to this article can be found online at https://doi.org/10.1016/j.scitotenv.2022.161374.

References

Ashmore, P.E., 1988. Bed load transport in braided gravel-bed stream models. Earth Surf. Process. Landf. 13 (8), 677–695. https://doi.org/10.1002/esp.3290130803.

Ashmore, P., Bertoldi, W., Tobias Gardner, J., 2011. Active width of gravel-bed braided rivers. Earth Surf. Process. Landf. 36 (11), 1510–1521. https://doi.org/10.1002/esp.2182.

Bakker, M., Antoniazza, G., Odermatt, E., Lane, S.N., 2019. Morphological response of an alpine braided reach to sediment-laden flow events. J. Geophys. Res. Earth Surf. https://doi.org/10.1029/2018JF004811.

Battin, T.J., Kaplan, L.A., Newbold, J.D., Cheng, X., Hansen, C., 2003. Effects of current velocity on the nascent architecture of stream microbial biofilms. Appl. Environ. Microbiol. 69 (9), 5443–5452. https://doi.org/10.1128/AEM.69.9.5443-5452.2003.

Battin, T.J., Wille, A., Psenner, R., Richter, A., 2004. Large-scale environmental controls on microbial biofilms in high-alpine streams. Biogeosciences 1 (2), 159–171.

Bertoldi, W., Zanoni, L., Tubino, M., 2009. Planform dynamics of braided streams. Earth Surf. Process. Landf. 34 (4), 547–557. https://doi.org/10.1002/esp.1755.

Biggs, B.J.F., Close, M.E., 1989. Periphyton biomass dynamics in gravel bed rivers: the relative effects of flows and nutrients. Freshw. Biol. 22 (2), 209–231. https://doi.org/10.1111/j.1365-2427.1989.tb01096.x.

Biggs, B.J.F., Smith, R.A., Duncan, M.J., 1999. Velocity and sediment disturbance of periphyton in headwater streams: biomass and metabolism. J. N. Am. Benthol. Soc. 18 (2), 222–241. https://doi.org/10.2307/1468462.

Boix Canadell, M., Gómez-Gener, L., Ulseth, A.J., Clémençon, M., Lane, S.N., Battin, T.J., 2021. Regimes of primary production and their drivers in alpine streams. Freshw. Biol. 66 (8), 1449–1463. https://doi.org/10.1111/fwb.13730.

Brandani, J., Peter, H., Busi, S.B., Kohler, T.J., Fodelianakis, S., Ezzat, L., Battin, T.J., 2022. Spatial patterns of benthic biofilm diversity among streams draining proglacial floodplains. Front. Microbiol. 13. https://doi.org/10.3389/fmicb.2022.948165.

Brasington, J., Rumsby, B.T., McVey, R.A., 2000. Monitoring and modelling morphological change in a braided gravel-bed river using high resolution GPS-based survey. Earth Surf. Process. Landf. 25 (9), 973–990. https://doi.org/10.1002/1096-9837(200008)25:9<973::AID-ESP111>3.0.CO;2-Y.

Brasington, J., Langham, J., Rumsby, B., 2003. Methodological sensitivity of morphometric estimates of coarse fluvial sediment transport. Geomorphology 53 (3), 299–316. https://doi.org/10.1016/S0169-555X(02)00320-3.

Chew, L.C., Ashmore, P.E., 2001. Channel adjustment and a test of rational regime theory in a proglacial braided stream. Geomorphology 37 (1–2), 43–63. https://doi.org/10.1016/S0169-555X(00)00062-3.

Egli, P.E., Irving, J., Lane, S.N., 2021. Characterization of subglacial marginal channels using 3-D analysis of high-density ground-penetrating radar data. J. Glaciol. 67 (264), 759–772. https://doi.org/10.1017/jog.2021.26.

Egozi, R., Ashmore, P., 2008. Defining and measuring braiding intensity. Earth Surf. Process. Landf. 33 (14), 2121–2138. https://doi.org/10.1002/esp.1658.

Egozi, R., Ashmore, P., 2009. Experimental analysis of braided channel pattern response to increased discharge. J. Geophys. Res. Earth Surf. 114 (F2). https://doi.org/10.1029/2008JF001099.

Francoeur, S.N., Biggs, B.J.F., 2006. Short-term effects of elevated velocity and sediment abrasion on benthic algal communities. Hydrobiologia 561 (1), 59–69. https://doi.org/10.1007/s10750-005-1604-4.

Gabbud, C., Robinson, C.T., Lane, S.N., 2019. Sub-basin and temporal variability of macroinvertebrate assemblages in alpine streams: when and where to sample? Hydrobiologia 830 (1), 179–200. https://doi.org/10.1007/s10750-018-3862-y.

Gerbersdorf, S.U., Manz, Werner, Paterson, D.M., 2008. The engineering potential of natural benthic bacterial assemblages in terms of the erosion resistance of sediments. FEMS Microbiol. Ecol. 66 (2), 282–294. https://doi.org/10.1111/j.1574-6941.2008.00586.x.

Gerbersdorf, S.U., Bittner, R., Lubarsky, H., Manz, W., Paterson, D.M., 2009. Microbial assemblages as ecosystem engineers of sediment stability. J. Soils Sediments 9 (6), 640–652. https://doi.org/10.1007/s11368-009-0142-5.

Germanoski, D., Schumm, S.A., 1993. Changes in Braided River morphology resulting from aggradation and degradation. J. Geol. 101 (4), 451–466. https://doi.org/10.1086/648239.

Gitelson, A.A., Kaufman, Y.J., Stark, R., Rundquist, D., 2002. Novel algorithms for remote estimation of vegetation fraction. Remote Sens. Environ. 80 (1), 76–87. https://doi.org/10.1016/S0034-4257(01)00289-9.

Gurnell, A.M., 1987. Fluvial sediment yield from alpine, glacierized catchments. In: Gurnell, A.M., Clark, M.J. (Eds.), Glacio-fluvial Sediment Transfer: An Alpine Perspective. John Wiley and Sons, New York, pp. 415–420.

Hawes, I., Howard-Williams, C., 1998. Primary production processes in streams of the mcmurdo dry valleys, Antarctica. Ecosystem Dynamics in a Polar Desert: The Mcmurdo Dry Valleys, Antarctica. American Geophysical Union (AGU), pp. 129–140 https://doi.org/10.1029/AR072p0129.

Heckmann, T., McColl, S., Morche, D., 2016. Retreating ice: research in pro-glacial areas matters. Earth Surf. Process. Landf. 41 (2), 271–276. https://doi.org/10.1002/esp.3858.

Hong, L.B., Davies, T.R.H., 1979. A study of stream braiding. Geol. Soc. Am. Bull. 90 (12_Part_II), 1839–1859. https://doi.org/10.1130/GSAB-P2-90-1839.

Horner, R.R., Welch, E.B., 1981. Stream periphyton development in relation to current velocity and nutrients. Can. J. Fish. Aquat. Sci. 38 (4), 449–457. https://doi.org/10.1139/f81-062.

Horner, R.R., Welch, E.B., Seeley, M.R., Jacoby, J.M., 1990. Responses of periphyton to changes in current velocity, suspended sediment and phosphorus concentration. Freshw. Biol. 24 (2), 215–232. https://doi.org/10.1111/j.1365-2427.1990.tb00704.x.

Howard, A.D., Keetch, M.E., Vincent, C.L., 1970. Topological and geometrical properties of braided streams. Water Resour. Res. 6 (6), 1674–1688. https://doi.org/10.1029/WR006i006p01674.

Hoyle, J.T., Kilroy, C., Hicks, D.M., Brown, L., 2017. The influence of sediment mobility and channel geomorphology on periphyton abundance. Freshw. Biol. 62 (2), 258–273. https://doi.org/10.1111/fwb.12865.

James, M.R., Robson, S., d'Oleire-Oltmanns, S., Niethammer, U., 2017. Optimising UAV topographic surveys processed with structure-from-motion: ground control quality, quantity and bundle adjustment. Geomorphology 280, 51–66. https://doi.org/10.1016/j.geomorph.2016.11.021.

James, M.R., Antoniazza, G., Robson, S., Lane, S.N., 2020. Mitigating systematic error in topographic models for geomorphic change detection: accuracy, precision and considerations beyond off-nadir imagery. Earth Surf. Process. Landf. 45 (10), 2251–2271. https://doi.org/10.1002/esp.4878.

Kawashima, S., Nakatani, M., 1998. An algorithm for estimating chlorophyll content in leaves using a video camera. Ann. Bot. 81 (1), 49–54. https://doi.org/10.1006/anbo.1997.0544.

Lane, S.N., Richards, K.S., 1997. Linking River Channel form and process: time, space and causality revisited. Earth Surf. Process. Landf. 22 (3), 249–260. https://doi.org/10.1002/(SICI)1096-9837(199703)22:3<249::AID-ESP752>3.0.CO;2-7.

Lane, S.N., Westaway, R.M., Murray Hicks, D., 2003. Estimation of erosion and deposition volumes in a large, gravel-bed, braided river using synoptic remote sensing. Earth Surf. Process. Landf. 28 (3), 249–271. https://doi.org/10.1002/esp.483.

Luce, J.J., Cattaneo, A., Lapointe, M.F., 2010. Spatial patterns in periphyton biomass after low-magnitude flow spates: geomorphic factors affecting patchiness across gravel–cobble riffles. J. N. Am. Benthol. Soc. 29 (2), 614–626. https://doi.org/10.1899/09-059.1.

Luce, J.J., Lapointe, M.F., Roy, A.G., Ketterling, D.B., 2013. The effects of sand abrasion of a predominantly stable stream bed on periphyton biomass losses: EFFECTS OF SAND ABRASION OF a STABLE STREAM BED ON PERIPHYTON BIOMASS LOSSES. Ecohydrology 6 (4), 689–699. https://doi.org/10.1002/eco.1332.

Maizels, J., 2002. 9—Sediments and landforms of modern proglacial terrestrial environments. In: Menzies, J. (Ed.), Modern and Past Glacial Environments. Butterworth-Heinemann, pp. 279–316 https://doi.org/10.1016/B978-075064226-2/50012-X.

Malard, F., Tockner, K., Ward, J.V., 1999. Shifting dominance of subcatchment water sources and flow paths in a glacial floodplain, val roseg, Switzerland. Arct. Antarct. Alp. Res. 31 (2), 135–150. https://doi.org/10.1080/15230430.1999.12003291.

Mancini, D., Lane, S.N., 2020. Changes in sediment connectivity following glacial debuttressing in an alpine valley system. Geomorphology 352, 106987. https://doi.org/10.1016/j.geomorph.2019.106987.

Marren, P.M., 2002. Glacier margin fluctuations, Skaftafellsjökull, Iceland: implications for Sandur evolution. Boreas 31 (1), 75–81. https://doi.org/10.1111/j.1502-3885.2002.tb01057.x.

Marren, P.M., 2005. Magnitude and frequency in proglacial rivers: a geomorphological and sedimentological perspective. Earth Sci. Rev. 70 (3), 203–251. https://doi.org/10.1016/j.earscirev.2004.12.002.

Marren, P.M., Toomath, S.C., 2013. Fluvial adjustments in response to glacier retreat: SkaftafellsjökullIceland. Boreas 42 (1), 57–70. https://doi.org/10.1111/j.1502-3885.2012.00275.x.

Marren, P.M., Toomath, S.C., 2014. Channel pattern of proglacial rivers: topographic forcing due to glacier retreat. Earth Surf. Process. Landf. 39 (7), 943–951. https://doi.org/10.1002/esp.3545.

Matthews, J., 1992. The Ecology of Recently-deglaciated Terrain. Cambridge University Press, Cambridge.

McKnight, D.M., Tate, C.M., Andrews, E.D., Niyogi, D.K., Cozzetto, K., Welch, K., Lyons, W.B., Capone, D.G., 2007. Reactivation of a cryptobiotic stream ecosystem in the McMurdo dry valleys, Antarctica: a long-term geomorphological experiment. Geomorphology 89 (1–2), 186–204. https://doi.org/10.1016/j.geomorph.2006.07.025.

Milan, D.J., Heritage, G.L., Large, A.R.G., Fuller, I.C., 2011. Filtering spatial error from DEMs: implications for morphological change estimation. Geomorphology 125 (1), 160–171. https://doi.org/10.1016/j.geomorph.2010.09.012.

Miller, H.R., Lane, S.N., 2019. Biogeomorphic feedbacks and the ecosystem engineering of recently deglaciated terrain. Prog. Phys. Geogr. Earth Environ. 43 (1), 24–45. https://doi.org/10.1177/0309133318816536.

Milner, A.M., Petts, G.E., 1994. Glacial rivers: physical habitat and ecology. Freshw. Biol. 32 (2), 295–307. https://doi.org/10.1111/j.1365-2427.1994.tb01127.x.

Mosley, M.P., 1982. Analysis of the effect of changing discharge on channel morphology and instream uses in a braided river, Ohau RiverNew Zealand. Water resources research 18 (4), 800–812. https://doi.org/10.1029/WR018i004p00800.

Müller, T., Lane, S.N., Schaefli, B., 2022. Towards a hydrogeomorphological understanding of proglacial catchments: an assessment of groundwater storage and release in an alpine catchment. Hydrol. Earth Syst. Sci. 26 (23), 6029–6054. https://doi.org/10.5194/hess-26-6029-2022.

Neumeier, U., Lucas, C.H., Collins, M., 2006. Erodibility and erosion patterns of mudflat sediments investigated using an annular flume. Aquat. Ecol. 40 (4), 543–554. https://doi.org/10.1007/s10452-004-0189-8.

Nienow, P., Sharp, M., Willis, I., 1998. Seasonal changes in the morphology of the subglacial drainage system, haut glacier d'ArollaSwitzerland. Earth Surface Processes and Landforms 23 (9), 825–843. https://doi.org/10.1002/(SICI)1096-9837(199809)23:9<825::AID-ESP893>3.0.CO;2-2.

Perolo, P., Bakker, M., Gabbud, C., Moradi, G., Rennie, C., Lane, S.N., 2019. Subglacial sediment production and snout marginal ice uplift during the late ablation season of a temperate valley glacier. Earth Surf. Process. Landf. 44 (5), 1117–1136. https://doi.org/10.1002/esp.4562.

Roncoroni, M., Lane, S.N., 2019. A framework for using small unmanned aircraft systems (sUASs) and SfM photogrammetry to detect salmonid redds. Ecol. Inform. 53, 100976. https://doi.org/10.1016/j.ecoinf.2019.100976.

Roncoroni, M., Brandani, J., Battin, T.I., Lane, S.N., 2019. Ecosystem engineers: biofilms and the ontogeny of glacier floodplain ecosystems. Wiley interdisciplinary reviewsWater 6 (6). https://doi.org/10.1002/wat2.1390.

Roncoroni, M., Mancini, D., Kohler, T.J., Miesen, F., Gianini, M., Battin, T.J., Lane, S.N., 2022. Centimeter-scale mapping of phototrophic biofilms in glacial forefields using visible band ratios and UAV imagery. International Journal of Remote Sensing 0 (0), 1–35. https://doi.org/10.1080/01431161.2022.2079963.

Roussel, E., Marren, P.M., Cossart, E., Toumazet, J.-P., Chenet, M., Grancher, D., Jomelli, V., 2018. Incision and aggradation in proglacial rivers: post-little ice age long-profile adjustments of southern Iceland outwash plains. Land Degrad. Dev. 29 (10), 3753–3771. https://doi.org/10.1002/ldr.3127.

Rydgren, K., Halvorsen, R., Töpper, J.P., Njøs, J.M., 2014. Glacier foreland succession and the fading effect of terrain age. J. Veg. Sci. 25 (6), 1367–1380. https://doi.org/10.1111/jvs.12184.

Swift, D.A., Nienow, P.W., Hoey, T.B., Mair, D.W.F., 2005. Seasonal evolution of runoff from haut glacier d'Arolla, Switzerland and implications for glacial geomorphic processes. J. Hydrol. 309 (1), 133–148. https://doi.org/10.1016/j.jhydrol.2004.11.016.

Thom, M., Schmidt, H., Gerbersdorf, S.U., Wieprecht, S., 2015. Seasonal biostabilization and erosion behavior of fluvial biofilms under different hydrodynamic and light conditions. Int. J. Sediment Res. 30 (4), 273–284. https://doi.org/10.1016/j.ijsrc.2015.03.015.

Uehlinger, U., Zah, R., Bürgi, H., 1998. The val roseg project: temporal and spatial patterns of benthic algae in an alpine stream. Hydrology, Water Resources and Ecology in Headwaters. 248, p. 419.

Uehlinger, U., Tockner, K., Malard, F., 2002. Ecological windows in glacial stream ecosystems. Eawag News [Engl. Ed.] 54, 20–21.

Uehlinger, U., Robinson, C.T., Hieber, M., Zah, R., 2010. The physico-chemical habitat template for periphyton in alpine glacial streams under a changing climate. Hydrobiologia 657 (1), 107–121. https://doi.org/10.1007/s10750-009-9963-x.

Warburton, J., Davies, T., 1994. Variability of bedload transport and channel morphology in a braided river hydraulic model. Earth Surf. Process. Landf. 19 (5), 403–421. https://doi.org/10.1002/esp.3290190503.

Ward, J.V., Burgherr, P., Gessner, M.O., Malard, F., Robinson, C.T., 1998. The val roseg project: habitat heterogeneity and connectivity gradients in a glacial flood-plain. Hydrology, water resources and ecology in headwaters. 248, p. 425.

Ward, J.V., Malard, F., Tockner, K., Uehlinger, U., 1999. Influence of ground water on surface water conditions in a glacial flood plain of the swiss Alps. Hydrol. Process. 13 (3), 277–293. https://doi.org/10.1002/(SICI)1099-1085(19990228)13:3<277::AID-HYP738>3.0.CO;2-N.